

Title	Stress Corrosion Cracking of SUS316 Stainless Steel in High Temperature Water(Materials, Metallurgy & Weldability)
Author(s)	Kuroda, Toshio; Kikuchi, Yasushi; Yeon, Yun Mo et al.
Citation	Transactions of JWRI. 1989, 18(1), p. 99-105
Version Type	VoR
URL	https://doi.org/10.18910/3800
rights	
Note	

Osaka University Knowledge Archive : OUKA

<https://ir.library.osaka-u.ac.jp/>

Osaka University

Stress Corrosion Cracking of SUS316 Stainless Steel in High Temperature Water†

Toshio KURODA*, Yasushi KIKUCHI**, Yun Mo YEON*** and Toshio ENJO****

Abstract

Effects of solution treatment temperature and sensitization time on stress corrosion cracking (SCC) have been studied on SUS316 stainless steel in high temperature water at 562K containing dissolved oxygen of 8ppm using a slow strain rate testing (SSRT) technique at $4.17 \times 10^{-6} \text{ s}^{-1}$ and $8.35 \times 10^{-7} \text{ s}^{-1}$. The Strauss test (ASTM A262E) and the oxalic acid etching test (ASTM A262A) were used to determine the degree of sensitization and Huey test (ASTM A262C) and anode polarization test were used to determine the influence of step solution treatment on segregation of impurities at grain boundary.

In the case of the specimens solution-treated at 1373K, $M_{23}C_6$ and Laves phases were many precipitated than that of the specimen solution-treated at 1573K. For the width of attacked grain boundaries, this trend was coincident. In high temperature water, intergranular corrosion was occurred owing to Cr depletion resulting from the precipitation of $M_{23}C_6$ and Laves phase at grain boundaries of sensitized specimens and then IGSCC was occurred at these attacked grain boundaries at the small amount of strain and load. IGSCC was propagated to TGSCC according to the increase of strain. It was considered that IGSCC hardly occurred owing to the decrease of Cr-depleted zone at grain boundaries resulting from the precipitation of Laves phases.

KEY WORDS: (Intergranular Corrosion) (Intergranular Stress Corrosion Cracking) (Sensitization) (Transmission Electron Microscopy) (Laves Phase) (Solution Temperature)

1. Introduction

Stress corrosion cracking of sensitized SUS304 stainless steel in high temperature water has been investigated comparing with intergranular corrosion, especially Cr depletion at the grain boundary¹⁻⁴). It is well known that SUS316 stainless steel has good resistance to corrosion comparing with SUS304 stainless steel, because of the Mo addition⁵). $M_{23}C_6$ and Mo compounds precipitate at the grain boundary for the sensitized SUS316 stainless steel⁶). However, the precipitation of these compounds has not been discussed comparing with SCC in high temperature water.

In this study, it was investigated that effects of solution treatment temperature and Mo on the precipitation behavior of $M_{23}C_6$ and SCC susceptibilities in high temperature water.

2. Experimental Procedures

Chemical compositions of SUS316 stainless steel are shown in Table 1. Samples were solution-treated at 1373K and 1573K in vacuum for 3.6ks, and then water-quenched. Solution-treated samples were sensitized at 973K for various times.

Table 1 Chemical composition of SUS316 stainless steel (mass%).

Material	C	Si	Mn	P	S	Ni	Cr	Mo	Fe
SUS 316	0.06	0.63	0.97	0.033	0.007	10.13	17.05	2.16	Bal.

Autoclave system and specimen size were as same as those of the previous report^{7,8}). SCC tests were carried out at crosshead speeds of $4.17 \times 10^{-6} \text{ s}^{-1}$ and $8.35 \times 10^{-7} \text{ s}^{-1}$ in high temperature water containing dissolved oxygen of 8 ppm at 562K under 8MPa. The dissolved oxygen content in water was automatically controlled by introducing N_2 and O_2 gas. The fracture surfaces of specimens were examined using scanning electron microscopy.

SCC susceptibility was evaluated by fracture strain and reduction in area (R.A.). Transmission electron microscopy was used to observe the carbides and Mo compounds. The degree of sensitization was evaluated using 10% oxalic acid test (ASTM A262A), Strauss test (ASTM A262E), Huey test (ASTM A262C) and pitting potential in 3.5% NaCl solution.

3. Results and Discussion

3.1 Effect of solution treatment temperature on precipitation of $M_{23}C_6$ and Laves phase.

Figure 1 shows microstructures of sensitized specimens

† Received on May 8, 1986

* Instructor

** Associate Professor

*** Graduate Student

**** Professor (deceased)

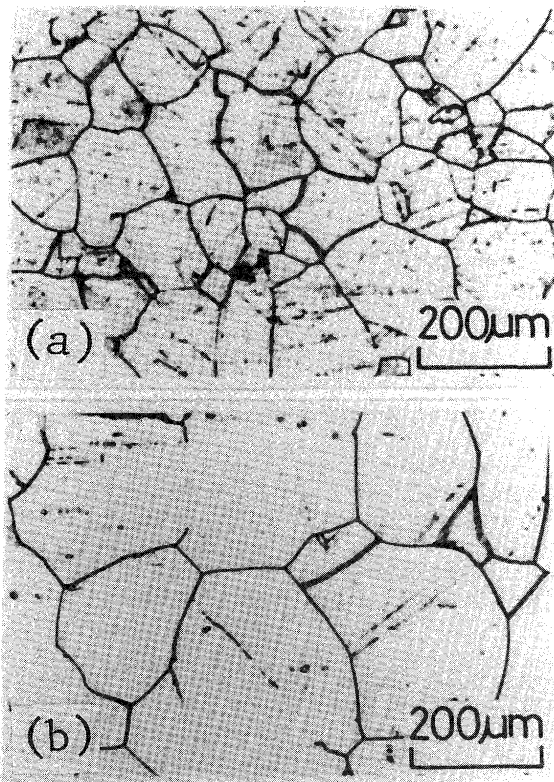


Fig. 1 Interganular corrosion in A262A test for specimens which were solutionized for 3.6ks at 1373K (a) and 1573K (b), and subsequently sensitized at 973K for 72ks.

after 10% oxalic acid test. In case of the specimen heat-treated at 1373K, grain boundaries were greatly attacked comparing with the specimen heat-treated at 1573K. However, the precipitates were not observed for the solution-treated specimen.

Figure 2 shows a transmission electron micrograph of the grain boundary precipitates for the specimens sensitized for 72ks. The grain boundary precipitates were identified to $M_{23}C_6$ and Laves phase. Laves phase is composing of Fe-Mo compounds.

Figure 3 shows transmission electron micrographs of the grain boundary precipitates for the specimen sensitized for 1015ks. Laves phases for the specimens heat-treated at 1373K were larger than those of the specimens heat-treated at 1573K.

Figure 4 shows a transmission electron micrograph of the precipitates in grain. The precipitates were identified as Laves phase. From these results, the precipitates in the photographs shown in Fig. 1 were $M_{23}C_6$ and Laves phases. Also, it means that $M_{23}C_6$ and Laves phase for the specimens heat-treated at 1373K precipitated more comparing with those of 1573K. It is considered that the precipitation of $M_{23}C_6$ is decreased by the precipitation of Laves phases.

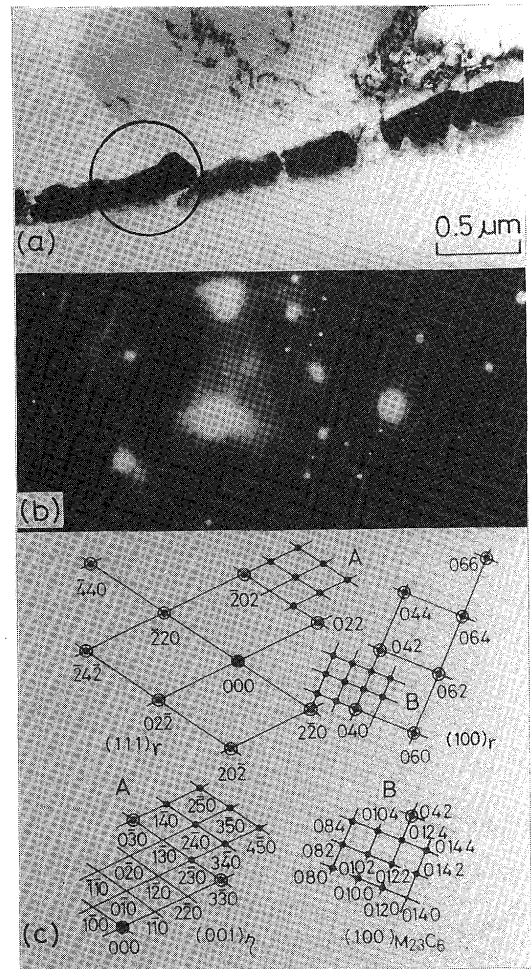


Fig. 2 Grain boundary precipitates in the specimen which was sensitized at 973K for 72ks after the solution treatment at 1373K for 3.6ks. (a): TEM micrograph (b), (c) Diffraction patterns

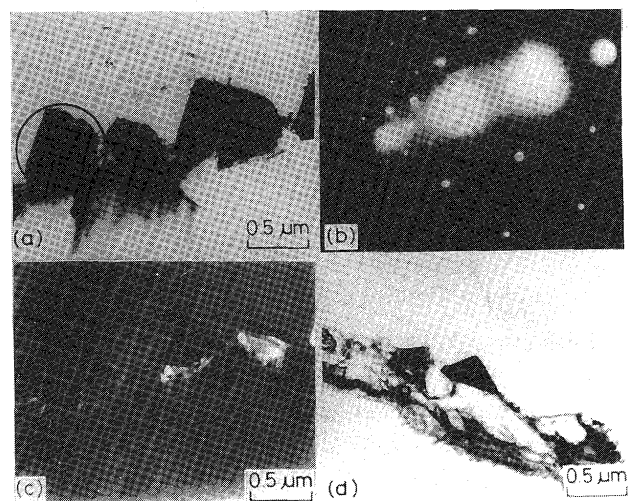


Fig. 3 Grain boundary precipitates in specimens which was sensitized at 973K for 1015ks after the solution treatment at 1373K (a) (b) (c) and 1573K (d). (a), (c), (d): TEM micrograph (b): Diffraction pattern

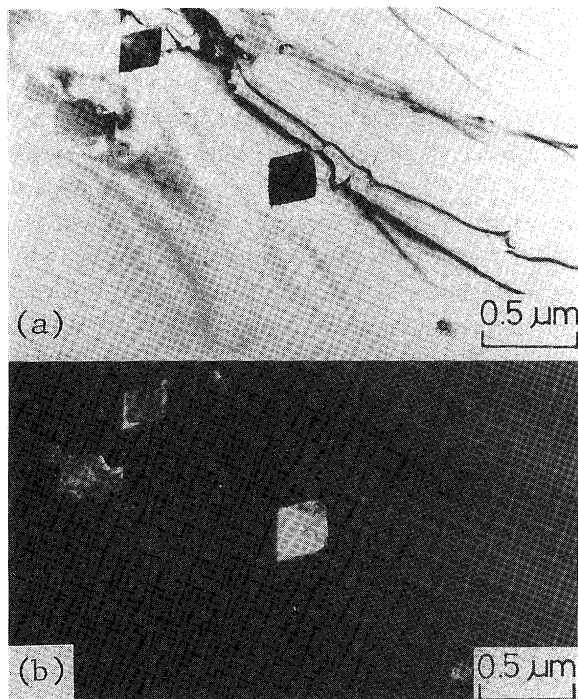


Fig. 4 Precipitates in a specimen sensitized at 973K for 1015ks after the solution treatment at 1573K.

3.2 Relation between precipitation behavior of $M_{23}C_6$, Laves phase and intergranular corrosion.

Figure 5 shows a relation between a degree of sensitization by means of A262A test and sensitization time⁹⁾. The degree of sensitization increased with increasing sensitization time. The degree of sensitization for the specimens heat-treated at 1373K is larger than those for the specimens heat-treated at 1573K. It is considered that the degree of sensitization is correlated with the precipitation of $M_{23}C_6$ and Laves phase. Cr depleted zones adjacent of $M_{23}C_6$ and Mo depleted zones adjacent to Laves phase were investigated.

Figure 6 shows the result of Strauss test. The widths of attacked grain boundaries increased with increasing sensitization time. It is considered that the growth of Laves phase is correlated with the drastic increase of widths of attacked grain boundaries. Because the Laves phase is Mo compounds containing 11%Cr-38%Fe, it is considered that Mo depleted zone affects intergranular corrosion susceptibility. Also, the widths of attacked grain boundary for the specimens heat-treated at 1373K were broader comparing with those of the specimens heat-treated at 1573K. It seems that these results are concerned with the attack of the regions adjacent to $M_{23}C_6$ and Laves phase. The precipitation of $M_{23}C_6$ and Laves phase for SUS316 stainless steel during sensitization treatment was similar to those of SUS304 stainless steel. It is considered that the change of precipitation by the solution treatment temper-

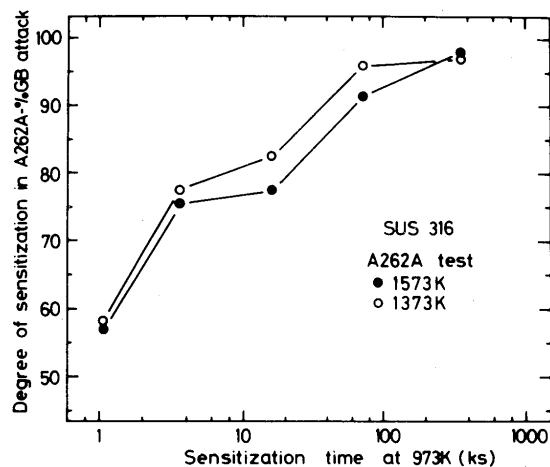


Fig. 5 Effect of sensitization time on the degree of G.B. attack in A262A test.

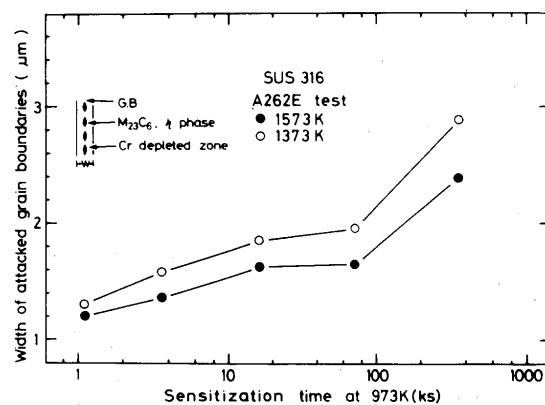


Fig. 6 Effect of sensitization time on the width of attacked region at grain boundaries in the Strauss test.

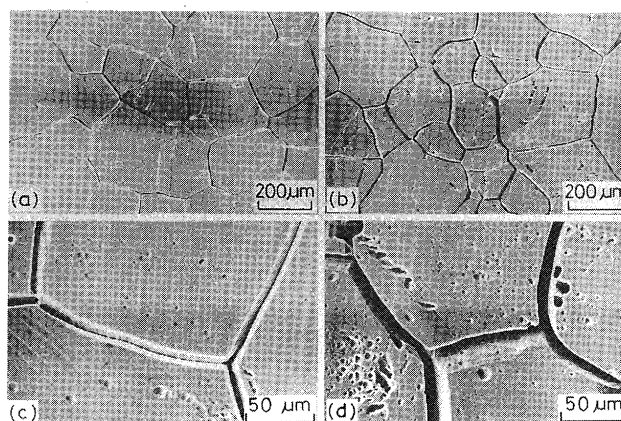


Fig. 7 Morphology of solutionized specimens after the Huey test.
 (a), (c): 1573K, 3.6ks W.Q.
 (b), (d): 1573, 3.6ks + 1373K, 72ks W.Q.

ature is correlated with the segregation of impurity at the grain boundary.

Figure 7 shows the surface appearance after Huey test for the solution-treated specimen. The grain boundary of the specimens held at 1373K for 72ks were greatly attacked comparing with those of the specimens heat-

treated at 1573K. It is considered that the intergranular attack increased owing to the segregation of impurity at the grain boundary.

Figure 8 shows the effect of holding time at 1373K on corrosion rate by Huey test. At any case of solution-treated specimens and sensitized specimens, the corrosion rate increased with increasing holding time at 1373K. Also, in case of the sensitized specimens, corrosion rate is 10 times larger than those of solution-treated specimens. It is considered that this increase of corrosion rate is correlated with the segregation of impurity and the precipitation of $M_{23}C_6$. Laves phase resulting from sensitization.

Figure 9 shows the effect of holding time at 1373K on pitting potential in 3.5%NaCl solution. At any case of solution-treated specimens and sensitized specimens, pit-

ting potential decreases with increasing holding time at 1373K. In case of the solution-treated specimens, the decrease of pitting potential was correlated with the segregation of impurity at the grain boundary. In case of the sensitized specimens, the pitting potential is about 100mV_{SCE} low at any holding time. These tendency is similar to that of corrosion rate in Huey test.

Figure 10 shows transmission electron micrographs of the grain boundary carbides for sensitized specimens. The grain boundary carbides of the specimen held at 1373K were larger than those of the specimen held at 1573K. From this result, it is considered that the impurity element segregated at the grain boundary accelerate the growth of $M_{23}C_6$ and Laves phase during sensitization.

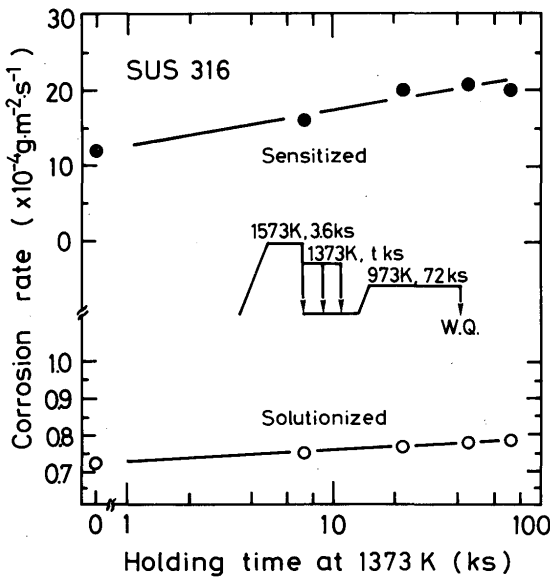


Fig. 8 Effect of holding time at 1373K on corrosion rate in the Huey test.

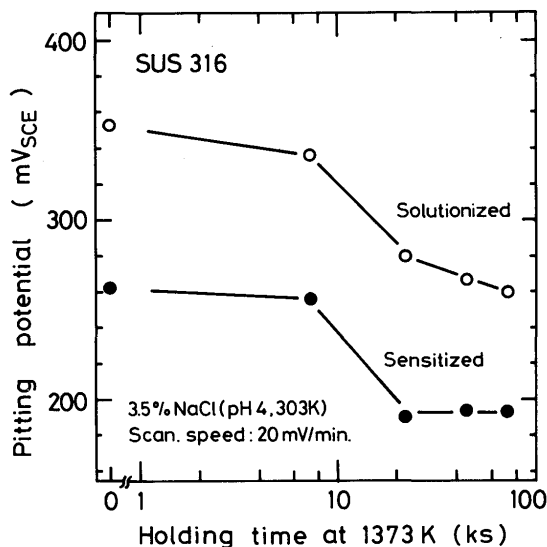


Fig. 9 Effect of holding time at 1373K on pitting potential.

3.3 Effects of solution treatment temperature and sensitization time on SCC susceptibility.

Figure 11 shows effects of solution treatment temperature and sensitization time on SCC susceptibility at the strain rate of $8.35 \times 10^{-7} s^{-1}$ in high temperature water. The reduction in area (R.A.) of sensitized specimens decreases with increasing sensitization time. However, R.A. increased at long time. That is, SCC did not occur at long time. This tendency was similar to the result of fracture strain. Also, SCC fraction and IGSCC fraction are correspondent with R.A. and fracture strain. However, SCC susceptibility of specimen heat-treated at 1373K is higher than that of specimen heat-treated at 1573K. It is

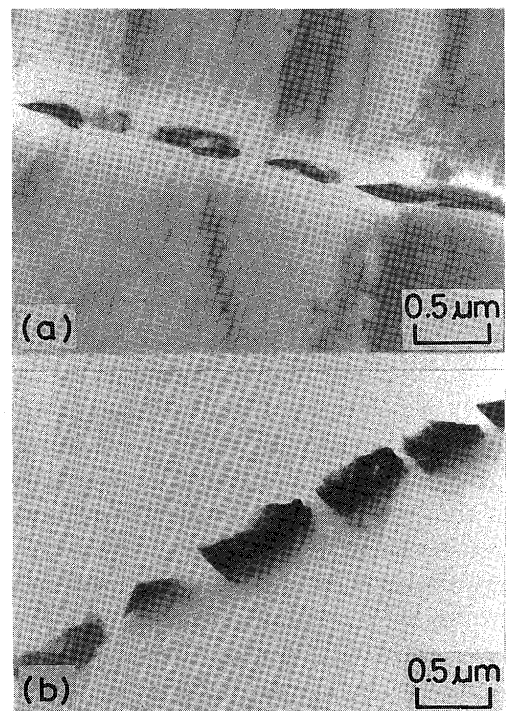


Fig. 10 Transmission electron micrographs of sensitized specimens solution-treated at 1573K for 1.8ks (a) and held at 1373K for 72ks after the solution treatment (b).

considered that the SCC susceptibility of SUS316 stainless steel is lower comparing with SUS304 stainless steel owing to the precipitation of Laves phase at the grain

boundary. That is, the precipitation of $M_{23}C_6$ is suppressed by the precipitation of Laves phase. Also, SCC susceptibility decreases at long sensitization time. It is considered that the decrease of SCC susceptibility is correlated with the healing of Cr in the Cr depleted zone and the decrease of precipitation of $M_{23}C_6$ resulting from the precipitation of Laves phase.

Figure 12 shows the SCC crack of sensitized specimens. In case of the specimens heat-treated at 1373K, it means that SCC crack initiated at the grain boundary and propagated along the grain boundary. However, in case of the

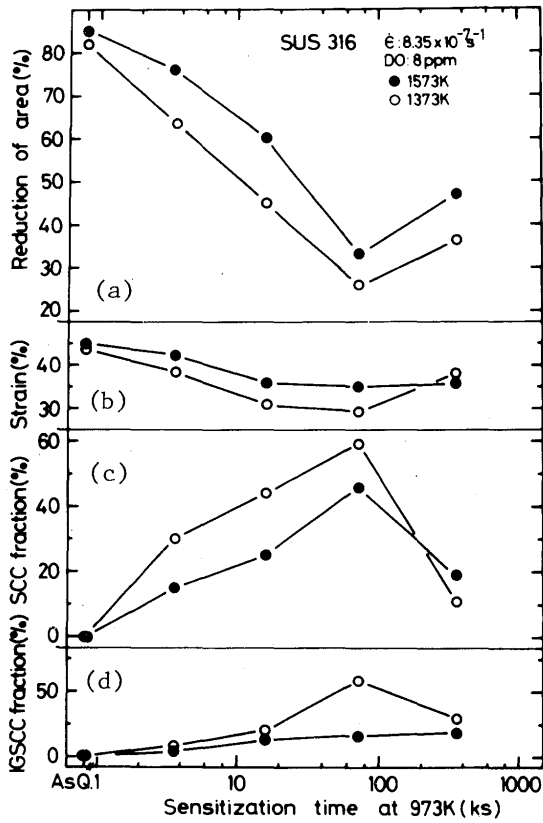


Fig. 11 Effect of sensitization time on SCC susceptibilities.

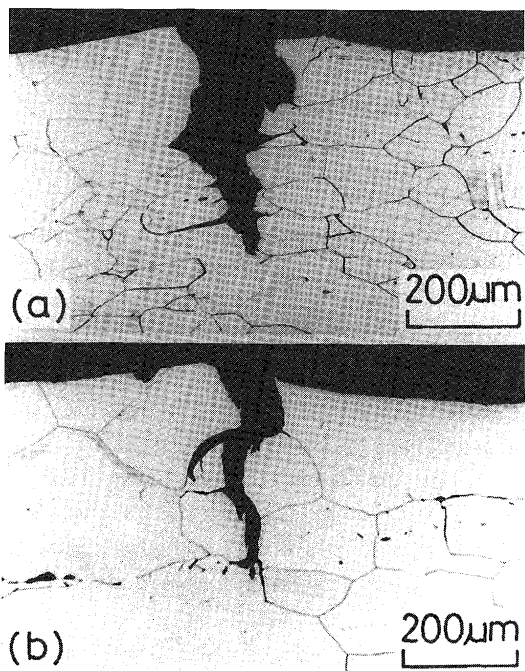


Fig. 12 Micrographs of longitudinal sections after SCC test for specimens sensitized at 973K for 72ks after the solution treatment at 1373K for 3.6ks(a), 1573K for 3.6ks(b).

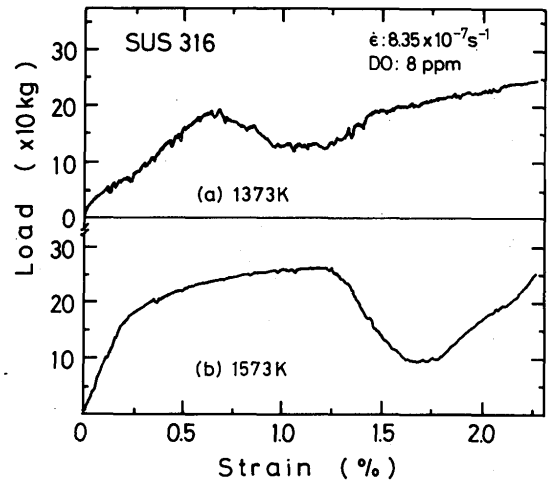


Fig. 13 Effect of solutionizing temperature on load-strain curves of specimens sensitized at 973K for 72ks after the solution treatment at 1373K (a) and 1573K (b) for 3.6ks.

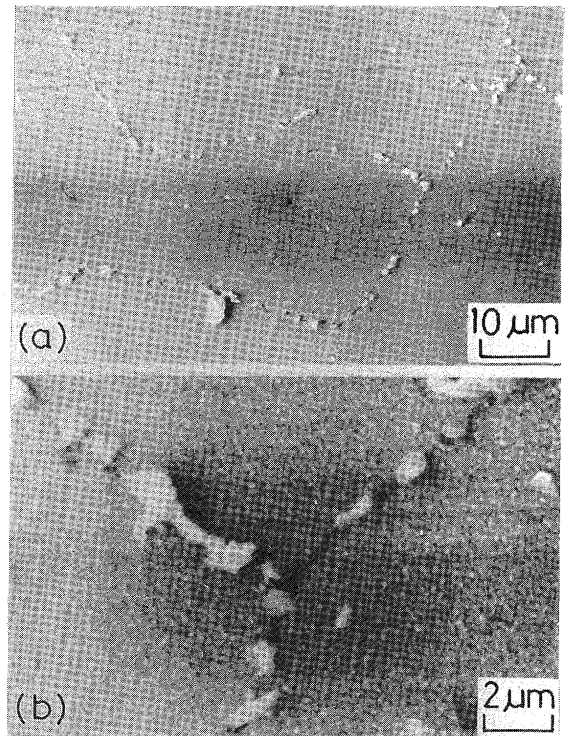


Fig. 14 Integranular corrosion of sensitized specimen immersed in water at 562K for 240ks.

specimens heat-treated at 1573K, it seems that the SCC crack initiated at the grain boundary and propagated into the grain. This tendency of the crack initiation and propagation of SUS316 stainless steel was similar to that of SUS304 stainless steel. It is considered that the initiation behavior of SCC crack is concerned with load-strain curve.

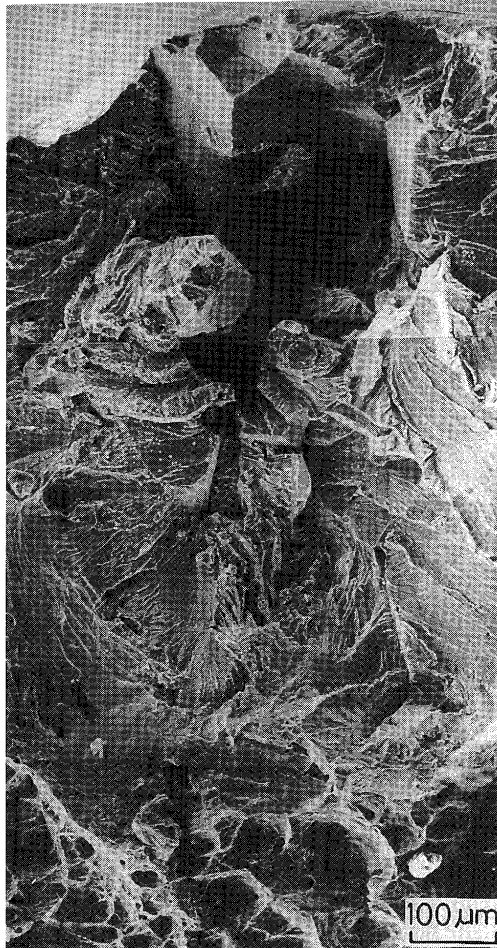


Fig. 15 Initiation and propagation of crack in SCC test for specimen sensitized at 973K for 3.6ks after the solution treatment at 1373K for 3.6ks.

Figure 13 shows the load-strain curves of sensitized specimens during SCC test in high temperature water. In case of the specimens heat-treated at 1373K, load decreases at the lower strain comparing with the specimens heat-treated at 1573K. It is considered that IGSCC initiates at the low strain. It was investigated on the specimen surface attacked in high temperature water in order to observe SCC initiation.

Figure 14 shows scanning electron micrographs of the specimen surfaces attacked in high temperature water. Corrosion products were observed at the grain boundary, but not pits. Consequently, SCC did not occur from the pits. It is considered that the pits hardly occur owing to Mo.

Figure 15 shows scanning electron micrographs of the typical fracture surface after SCC test. SCC was initiated at the grain boundary near the specimen surface and propagated into grain with fan-shaped pattern. At last, the specimens was fractured mechanically. From this fracture surface, it is considered that this intergranular fracture pattern are coincident with the decrease of the load as shown in Fig. 13.

Figure 16 shows schematic illustration of the precipitation of $M_{23}C_6$. Laves phase and SCC crack. In case of the solution-treated specimens, SCC did not occur owing to nothing of Cr depleted zone. However, in case of the sensitized specimens, SCC initiated and propagated along the grain boundary owing to Cr and Mo depleted zones resulting from the precipitation of $M_{23}C_6$ and Laves phase. Also, in case of the long time sensitized specimens, SCC initiated at grain boundary. But, its cracks propagated to grain not to grain boundary. It is considered that the decrease of SCC susceptibility is concerned with the decrease of Cr depleted zone resulting from Cr healing.

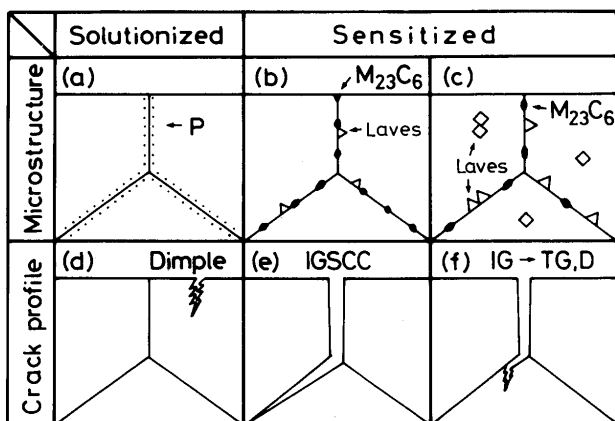


Fig. 16 Schematic diagram illustrating the microstructure and crack profile in SCC test.

4. Conclusion

In this study, it was investigated that the effects of solution treatment temperature and sensitization at 973K on SCC susceptibility of SUS316 stainless steel in high temperature water. Also, the precipitation behavior of $M_{23}C_6$ and Laves phase was compared with intergranular corrosion test. The results obtained in this study are summarized as follows.

- 1) In case of the sensitized specimens, Laves phase precipitated with $M_{23}C_6$. In case of the specimens heat-treated at 1373K, $M_{23}C_6$ and Laves phase precipitated more comparing with the specimens heat-treated at 1573K.
- 2) The width of attacked grain boundary increased with increasing sensitization time. Also, the width of specimens heat-treated at 1373K was broader comparing with that of the specimens heat-treated at 1573K.

- 3) In case of the step-solution treated specimens, the width of attacked grain boundary in the Huey test increased with increasing holding time at 1373K. It means that this increase of width of attacked grain boundary is concerned with the segregation of impurity at the grain boundary.
- 4) The precipitation of $M_{23}C_6$ and Laves phase increased with increasing holding time at 1373K. It is considered that the impurities segregated at the grain boundary accelerate the growth of $M_{23}C_6$ and Laves phase during sensitization treatment.
- 5) In case of the specimens heat-treated at 1373K, SCC susceptibility was higher than that of the specimens heat-treated at 1573K. This susceptibility was coincident with the precipitation behavior of $M_{23}C_6$ and Laves phase at the grain boundary and intergranular corrosion susceptibility. From these results, it is considered that the precipitation of Laves phase at the

grain boundary suppress the precipitation of $M_{23}C_6$ and SCC susceptibility decreases owing to the decrease of Cr depleted zone.

References

- 1) Y. Mukai, M. Murata, N. Tamaoki and H. Kazaoka: Quart. J. of Japan Weld. Soc., 3-2, (1985), 422 (In Japanese).
- 2) Y. Mukai and M. Murata: J. of Soc. of Mat. Sci. Japan, 34-381, (1985), 697 (In Japanese).
- 3) C.L. Briant and E.L. Hall: Corrosion, 42-9, (1986), 522.
- 4) R.A. Mulford, E.L. Hall and C.L. Briant: Corrosion, 39-4, (1983), 132.
- 5) M. Kowaka: "Kinzoku no Fussyoku Sonshou to Bousyoku Gjutu", Agne, (1983) (In Japanese).
- 6) B. Weiss and R. Stickler: Metall. Trans. 3A-4, (1972), 851.
- 7) T. Enjo, T. Kuroda and Y.M. Yeon: Quart. J. of Japan Weld. Soc., 4-1 (1986), 109 (In Japanese).
- 8) T. Enjo, T. Kuroda and Y.M. Yeon: Quart. J. of Japan Weld. Soc., 5-4 (1987), 516.
- 9) H.D. Solomon: Corrosion, 40-2, (1984), 51.